

Novel isoquinolone PDK1 inhibitors discovered through fragment-based lead discovery

M. Catherine Johnson · Qiyue Hu · Laura Lingardo ·
Rose Ann Ferre · Samantha Greasley · Jiangli Yan ·
John Kath · Ping Chen · Jacques Ermolieff · Gordon Alton

Received: 20 April 2011 / Accepted: 28 June 2011 / Published online: 22 July 2011
© Springer Science+Business Media B.V. 2011

Abstract Phosphoinositide-dependent kinase-1 (PDK1) is a critical enzyme in the PI3K/AKT pathway and to the activation of AGC family protein kinases, including S6K, SGK, and PKC. Dysregulation of this pathway plays a key role in cancer cell growth, survival and tumor angiogenesis. As such, inhibitors of PDK1 offer the promise of a new therapeutic modality for cancer treatment. Fragment based drug screening has recently become a viable entry point for hit identification. In this work, NMR spectroscopy fragment screening of PDK1 afforded novel chemotypes as orthogonal starting points from HTS screening hits. Compounds identified as hits by NMR spectroscopy were tested in a biochemical assay, and fragments with activity in both assays were clustered. The Pfizer compound file was mined via substructure and 2D similarity search, and the chemotypes were prioritized by ligand efficiency (LE), SAR mining, chemical attractiveness, and chemical enablement of promising vectors. From this effort, an isoquinolone fragment hit, **5** (IC₅₀ 870 μM, LE = 0.39), was identified as a novel, ligand efficient inhibitor of PDK1 and a suitable

scaffold for further optimization. Initially in the absence of crystallographic data, a fragment growing approach efficiently explored four vectors of the isoquinolone scaffold via parallel synthesis to afford a compound with crystallographic data, **16** (IC₅₀ 41.4 μM, LE = 0.33). Subsequent lead optimization efforts provided **24** (IC₅₀ 1.8 μM, LE = 0.42), with greater than fivefold selectivity against other key pathway kinases.

Keywords Isoquinolone · PDK1 inhibitors · Fragment based lead discovery · Ligand efficiency

Abbreviations

| | |
|------|---------------------------------------|
| PDK1 | Phosphoinositide-dependent kinase-1 |
| PI3K | Phosphoinositide 3-kinase |
| LE | Ligand efficiency |
| HTS | High throughput screening |
| MW | Molecular weight |
| STD | Saturation transfer difference |
| NO | Nitrogen and oxygen count |
| TPSA | Total polar surface area |
| HBD | Hydrogen bond donor count |
| SSHE | Substructure similarity hit expansion |

Introduction

Fragment based screening and ligand optimization has recently become a valuable and important new discovery tool in the arsenal of any drug discovery program and is now viewed as a viable complementary starting point to HTS for finding lead material to prosecute on many projects. Several excellent reviews cover various aspects of the fragment based approaches and techniques [1–4]. During fragment screening, small libraries of low molecular

M. C. Johnson (✉) · Q. Hu · L. Lingardo ·
R. A. Ferre · S. Greasley · J. Yan · J. Kath · P. Chen ·
J. Ermolieff · G. Alton
Pfizer Global Research and Development, 10770 Science Center
Drive, San Diego, CA 92121, USA
e-mail: mcjohnson@inchemdesign.com

Present Address:
M. C. Johnson
Integrated Chemistry Design, Inc., 3930 Stanford Dr, Oceanside,
CA 92056, USA

Present Address:
G. Alton
Visionary Pharmaceuticals, 11555 Sorrento Valley Road Suite
A, San Diego, CA 92121, USA

weight ($MW < 300$) compounds are screened against a target by sensitive biophysical techniques to find weak to moderate binding ligands. Two key advantages differentiate Fragment-Based Lead Discovery from other techniques [5]. First, the broader sampling of potential chemical space provides increased hit rates for low complexity molecules that are also excellent lead optimization starting points. With higher hit rates, project teams can prosecute more scaffolds with orthogonal risk profiles. Secondly, fragments can often provide a better lead optimization starting point since the ligand efficiency [6]¹ is comparable if not higher than larger hit molecules.

PDK1 (phosphoinositide-dependent kinase-1) is a member of the AGC serine/threonine kinase family that functions downstream from phosphoinositide 3-kinase (PI3K). It is called a “master regulator” because it phosphorylates highly conserved serine or threonine residues in the T-loop of at least 23 related downstream AGC protein kinases including PKB/Akt, p70S6K1, SGK, RSK and PKC [7–9]. These AGC protein kinases are integral to regulating a number of physiological processes, i.e. metabolism, growth, cell proliferation and survival. More than 50% of all common human cancers including breast, lung, prostate and blood possess overstimulation of the PDK1 signaling pathway [7]. A recent mouse study finds that decreasing the expression of PDK1 in $PTEN^{+/-}$ mice protected these animals from developing a wide range of tumors [10]. These combined data suggest that inhibitors of PDK1 could potentially provide a therapeutic cancer treatment. A review reports of several classes of small molecule inhibitors of PDK1 [7], and more recent disclosures include a wide variety of scaffolds [11–13]. Fragment based screening approaches to discover inhibitors of PDK1 are also described [14–17].

Results and discussion

To complement our HTS screen efforts, a fragment based screening effort was pursued to find new lead matter with an orthogonal risk profile for a PDK1 project. The generalized strategy for our overall efforts involved the process outlined in the flowchart (Fig. 1). A NMR fragment screening approach was selected to initiate the study where fragments were tested at a concentration of 300 μM . The aim of the study was to find both inhibitors that would bind to the traditional ATP pocket as well as the PIF pocket sites, and the methods used for the screening campaign as well as the PIF pocket ligands have been fully described [18]. At the time the screen was completed, the Pfizer fragment library consisted of 10,237 diverse, low molecular weight

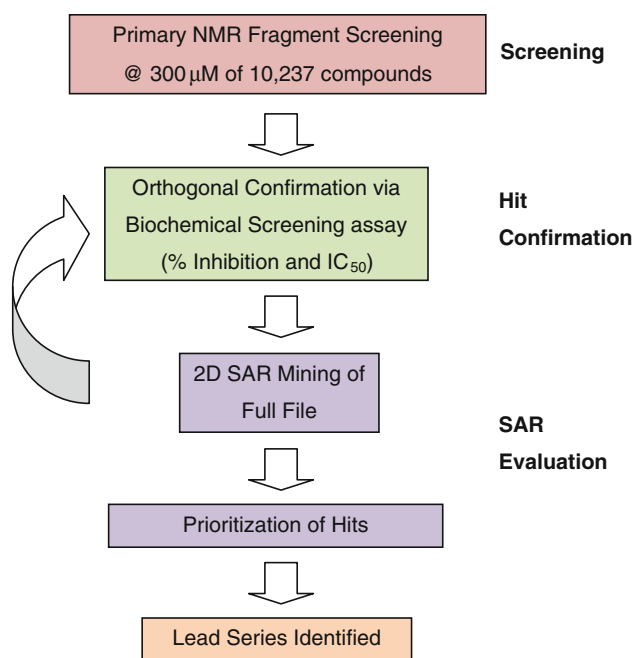


Fig. 1 Fragment-based screening strategy

fragments, assembled from the proprietary compound collection and commercial sources.

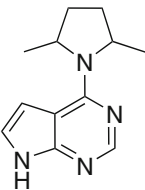
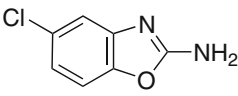
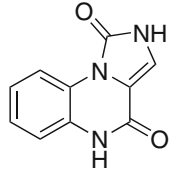
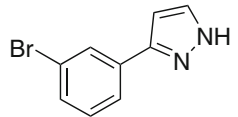
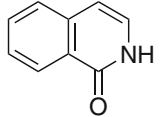
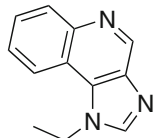
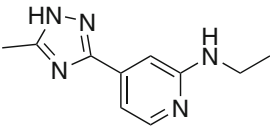
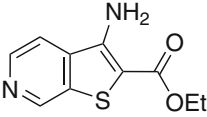
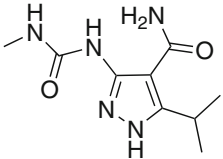
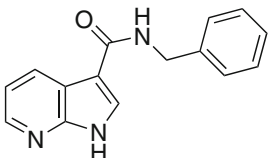
From the initial NMR screening, 370 ligands were identified and confirmed as hits to give a 3.6% hit identification rate. These hits were tested in an orthogonal biochemical kinase assay at high fragment concentration, 400 μM ². Since testing resources were limited, hits were defined as having a percent inhibition $\geq 30\%$ @ 400 μM , and 38 compounds met this criterion, providing a 10% confirmation rate between the NMR and biochemical screening techniques. The IC_{50} 's of the 38 ranged from 20 to 870 μM , and 19 had calculated ligand efficiency (LE) > 0.3 [6, See footnote 1]. The 19 compounds were clustered, and these 19 were spread across 10 distinct chemical classes, shown in decreasing LE (Table 1). Each of these 10 fragments was also tested in an NMR ATP competition study, and all were confirmed to be ATP competitive, except for **10**. The Saturation Transfer Difference (STD) intensities of ATP [3, 19] were monitored in the absence and in the presence of the 10 fragments, and all except **10** exhibited $> 50\%$ change measured, indicating that they are all ATP competitive except for **10**.

The proprietary collection was mined using the ten classes of compounds via substructure and 2D similarity methods using the Accord Chemistry Cartridge from

¹ Ligand efficiency (LE) is defined as $\Delta G/N_{\text{non-hydrogen atoms}}$, where $\Delta G \approx -RT \ln IC_{50}$.

² Kinase-Glo Assay (Promega Corporation) detects amount of ATP remaining after kinase reaction is stopped, thereby indirectly measuring PDK1 mediated phosphorylation of peptide substrate with [PDKtide] = 8 μM , [ATP] = 5 μM , and [PDK1 enzyme] = 15 nM. Details are given in [18].

Table 1 PDK1 ^1H NMR fragment screening hits

| Structure | Compound | MW | PDK1 IC_{50} (μM) | LE | ATP competitive |
|---|-----------|--------|---|------|-----------------|
|  | 1 | 216.28 | 20.7 | 0.42 | + |
|  | 2 | 168.58 | 863 | 0.41 | + |
|  | 3 | 201.18 | 66.6 | 0.40 | + |
|  | 4 | 223.07 | 705 | 0.39 | + |
|  | 5 | 145.16 | 870 | 0.39 | + |
|  | 6 | 197.24 | 230 | 0.35 | + |
|  | 7 | 203.24 | 365 | 0.34 | + |
|  | 8 | 222.26 | 504 | 0.32 | + |
|  | 9 | 225.25 | 310 | 0.32 | + |
|  | 10 | 251.28 | 123 | 0.30 | – |

Accelrys [20]. The results for each of the substructure and similarity searches were filtered for MW <300, NO (Nitrogen and Oxygen count) <8, TPSA (total polar surface area) <120, clogD <4.5, and HBD (hydrogen bond donor count) <3. The combined culled lists from the mining exercises were submitted for % Inhibition testing in the biochemical assay, and those meeting the cutoff requirements, $\geq 30\%$ Inhibition @ 400 μM , were followed-up in the IC_{50} assay. With limited chemistry resources, not all of the chemical classes could be pursued within a reasonable timeframe, so a pragmatic approach guided the rationale for the prioritization strategy. Follow-up work for the compound classes was prioritized using the following criteria, in roughly decreasing level of importance:

1. Calculated LE for compound class
2. Chemical Attractiveness
3. SAR mining (2D brother/sister mining)
4. Robust chemical enablement of cores with promising vectors.

First, the calculated LE for a compound class was given the highest priority. A recent article from Hajduk [21] highlighted the importance of starting the fragment optimization process with the most LE lead, since efficiency often remained constant during lead optimization, and a suboptimal fragment lead could further complicate the challenging optimization task of balancing solubility, permeability and stability. For this project, LE was used as a quantitative measure of the effectiveness of the fragment elaboration during the optimization process [21]. Chemical attractiveness, often a subjective ranking term, was used to identify cores requiring major, time-consuming structural manipulation to remove unattractive features, while SAR mining verified the viability of a fragment core and provided insight into chemical enablement. Finally, the fragment core had to have promising vectors for fragment growing and facile chemical enablement to receive higher priority.

Using these guidelines, the ten compound classes were ranked. First, those compounds with higher LE were given higher ranking. Coincidentally, **1**, the most LE and attractive core, had also been identified during the HTS campaign, and this chemical series was already being pursued by other members of the project team. Few examples of related compounds to **3**, **6** and **9** were found, and these cores required major structural manipulations to remove unattractive features of the core. SAR mining for compounds **2**, **4**, **7**, and **8**, did not provide additional similar compounds with tractable SAR, so these series were discontinued. The azaindole amide compound, **10**, was heavily pursued via combinatorial exploration. Results from this exercise provided no compounds with greater potency or LE than **10**. For these reasons, these series were deprioritized. The isoquinolone, **5**, fragment, on the other hand, met all the criteria above. This

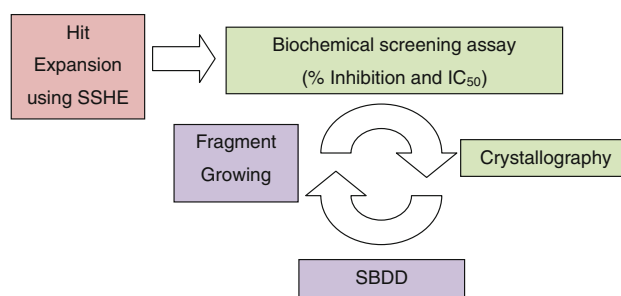


Fig. 2 Fragment-based lead optimization strategy

core had good LE, provided good SAR mining, and was chemically attractive, with promising vectors that were readily chemically accessible. The isoquinolone core was identified as having the best potential for further development, so efforts focused on advancing this series.

Expansion of the lead series involved the outlined workflow (Fig. 2). First, a 2D hit expansion tool named Substructure Similarity Hit Expansion (SSHE) was created to do the following tasks within a single workflow:

- (1) Expanded hits based on substructure and/or similarity searches against the full Pfizer file as well as commercially available compound file
- (2) Filtered results by various properties including: 2D similarity, logP, MW, number of atoms, number of hydrogen bond donors, number of hydrogen bond acceptors, number of rotatable bonds, and polar surface area (PSA)
- (3) Checked sample inventory availability
- (4) Created the hit list for screening.

The query set was also augmented by additional tautomeric enumeration. For example, in the case of the isoquinolone core, the corresponding 1-hydroxyisoquinoline was also included in the search. SSHE included the capability to simultaneously handle a large input hit list, to perform various filtering operations, and to return to the user a single combined result file. SSHE was implemented using Pipeline Pilot version 7.0 and was made easily accessible to bench chemists through webport technology [22]. Identified compounds were submitted for testing in the biochemical assay, and those with sufficient potency were sent for crystallographic determination. Analysis of the crystal structure data provided the insight for fragment growing using SBDD where combinatorial synthesis efforts were emphasized for ease of creating families of compounds with SAR.

Hit expansion effort using SSHE for the isoquinolone structure proved to be extremely productive. From these efforts, 6 and 7-bromoisquinolones, **11** and **12**, had improved potency and LE over the parent fragment, **5** (Fig. 3). In addition, compound **13**, and several similar compounds, provided further confirmation of the viability of the isoquinolone class and demonstrated the feasibility

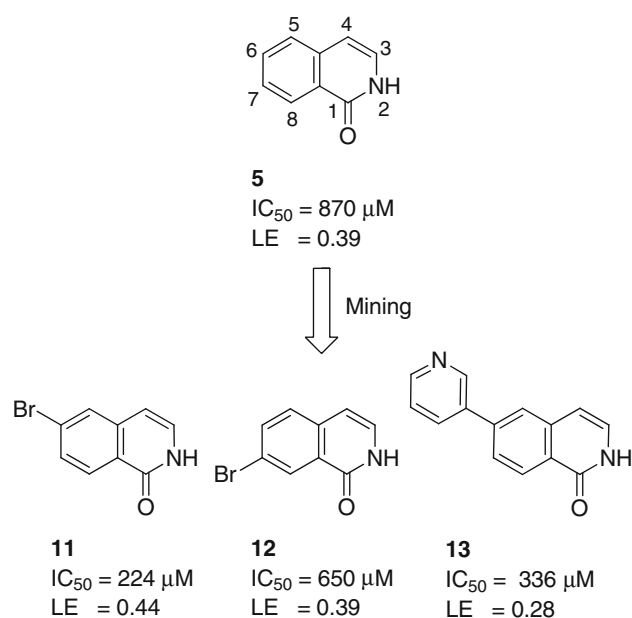


Fig. 3 Representative isoquinolone mining results

of growing the isoquinolone core at various vectors. Upon inspection, **13** was clearly derived from **11** via a simple Suzuki coupling reaction, so a simple route to exploring the chemical space around the isoquinolone core was also accessible. The isoquinolone core became the main focus of the lead optimization effort.

At the beginning of the project, the co-crystal structure of PDK1 with ATP was publically available (PDB code 1H1W) and provided valuable insight into the potential binding process of PDK1 with the isoquinolone fragment (Fig. 4). In this structure, the hinge binding consisted of a pair of key hydrogen bonds formed between the N1 N and

the C6 amino group of adenine with the backbone carbonyl oxygen of Ser-160 and the backbone NH of Ala-162. The N7 N also established a hydrogen bond with a key H₂O that bridged the phosphate backbone. Additional hydrogen bonds were observed between the phosphate and Ser-92 and Ser-94, and key interactions with the catalytic Lys-111 and Thr-222 were also seen.

Past fragment lead optimization campaigns had been most productive when structural information of the particular fragment of interest bound to the target protein was obtained. With a verified binding mode of the fragment, the fragment optimization process was greatly accelerated [5]. Efforts to obtain a crystal structure of **5** bound to PDK1 were inconclusive, so docking and scoring methods that ranked interactions of a ligand in the ATP pocket of a known PDK1 protein crystal structure were used to guide the lead optimization. Specifically, AGDOCK [23, 24] was employed as the docking and scoring engine while HT-Score [25] provided the associated protein–ligand scoring function.

From the ATP competition study, the isoquinolone fragment was known to be ATP competitive, so the isoquinolone was most likely interacting with the hinge region via Ser-160 and Ala-162. Analysis of the flat isoquinolone structure led to two likely binding modes. In the first proposed binding mode (Fig. 5), the isoquinolone would form a pair of key hydrogen bonds between the carbonyl O of the isoquinolone with the backbone NH of the Ala-162 and the N2 N of the isoquinolone with the backbone carbonyl of Ala-162. In this “flipped out” orientation, the isoquinolone was positioned closer to the solvent edge. In the alternative proposed binding mode (Fig. 6), the isoquinolone would establish a pair of key hydrogen bonds between the carbonyl O of the isoquinolone with the backbone NH of the Ala-162 and the N2 N of the isoquinolone with the backbone

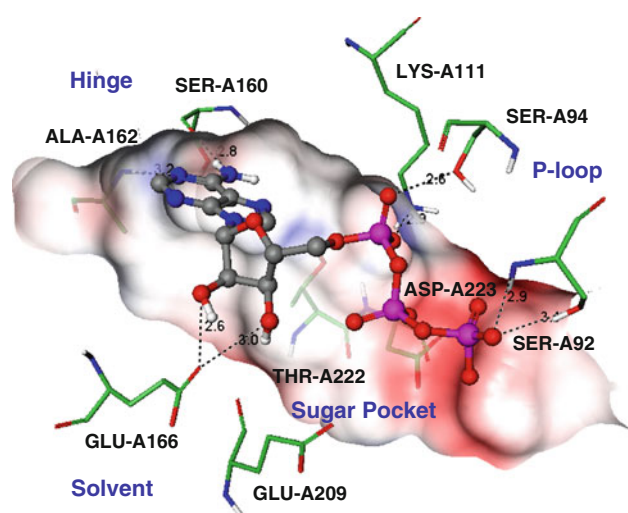


Fig. 4 X-Ray crystal structure of ATP bound to PDK1 (PDB code 1H1W)

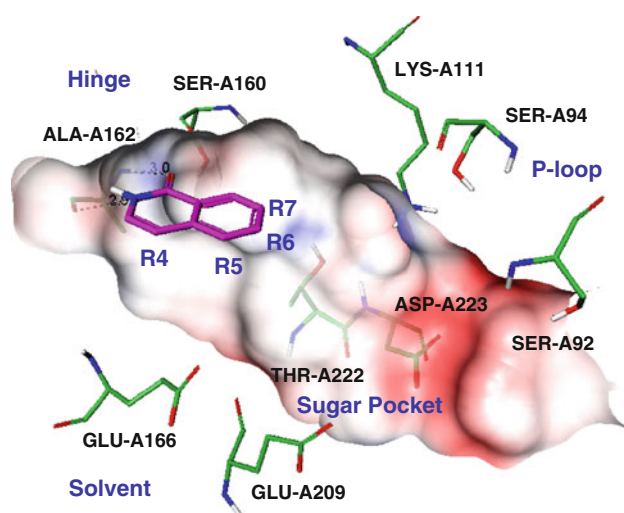


Fig. 5 “Flipped Out” binding mode with core positioned closer to solvent edge

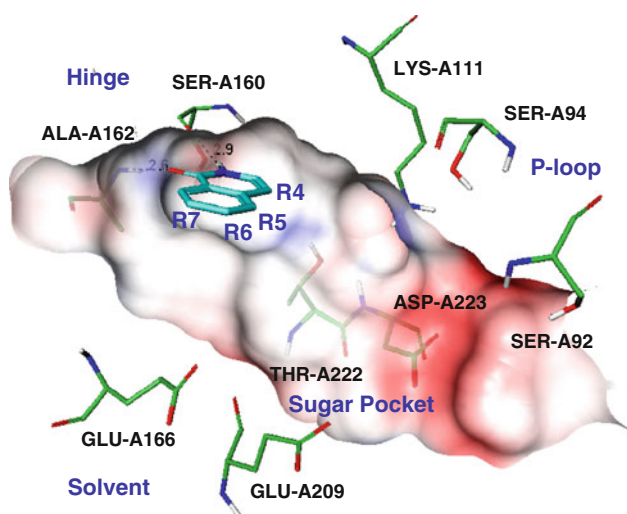


Fig. 6 “Flipped In” binding mode with core sitting further back in the pocket

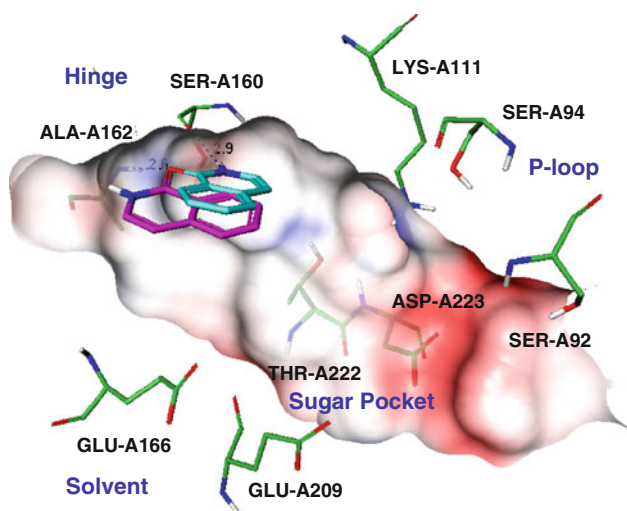


Fig. 7 Overlay of the two proposed isoquinolone binding modes, with the “Flipped In” shown in cyan and the “Flipped Out” shown in magenta

carbonyl of Ser-160. In this “flipped in” orientation, the isoquinolone was seated further back in the hinge.

From the overlay of the two proposed isoquinolone binding modes (Fig. 7), comparison was made of the residues and protein features to be targeted via vector growth (Table 2). It was anticipated that synthetic exploration of each of the vectors would provide an optimized compound for crystallographic determination that would allow determination of the binding mode for the isoquinolone core with PDK1. Although in both binding modes, the R_5 and R_6 vectors were predicted to provide favorable interactions between the ligand and the protein, the R_6 vector targeted the same key residues with either binding orientation, i.e. the sugar pocket and Asp-223. Compounds that explored

the R_4 or R_7 vectors effectively discriminated between the two binding modes, since these vectors tested the size limitations of each of the binding modes. Therefore, exploration off of the R_6 and R_7 positions was first pursued to find compounds with improved potency and to explore the size limitations for R_7 .

The goal for the synthesis exploration was to advance the isoquinolone series by increasing potency and maintaining LE but also to provide compounds with solubility $>100 \mu\text{M}$ to enable crystallography. Since the exploration off of each vector could be easily achieved in a single-step reaction, the strategy involved exploring the R_4 , R_5 , R_6 and R_7 vectors by Suzuki coupling, phenol alkylation, reductive amination, and amide formation with the simplest examples of each reaction shown for R_5 vector growth (Fig. 8). The precursor isoquinolones were readily prepared in 10 g scale through the preparation of acyl azides from cinnamic acids followed by thermal rearrangement to afford the desired isoquinolones [26].

With the starting isoquinolones in hand, combinatorial libraries were designed for each of the vectors for the four reaction types. Design criteria included the following calculated physical property parameters: MW <450 , number of hydrogen bond donors (HBD) <3 , clogP <4.5 , NO (Nitrogen & Oxygen count) <8 , and number of rotatable bonds (NRB) <8 . Each of the libraries was docked and scored in available PDK1 crystal structures. Final library designs were based on docking scores and physical property calculations, and privileged pieces from other PDK1 active compounds were included in the designs. Hits were defined as having $\geq 30\%$ Inhibition @ $400 \mu\text{M}$. Of the four reaction types, the amide coupling provided the least potent and LE compounds (Fig. 9). The reductive amination and

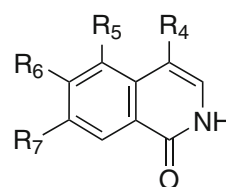


Table 2 Isoquinolone binding mode comparison with targeted residues

| | R_4 | R_5 | R_6 | R_7 |
|-----------------------|------------------------------|--------------------------------|-----------------------|----------------------------|
| Flipped Out (magenta) | Glu-166; solvent | Sugar pocket/ solvent; Glu-209 | Sugar pocket; Asp-223 | Very small groups; Thr-222 |
| Flipped In (cyan) | Small-medium groups; Thr-222 | Good access to the G-loop | Sugar pocket; Asp-223 | Glu-166; solvent |

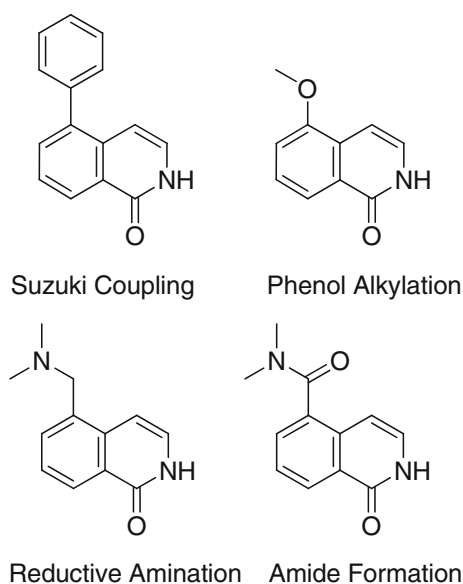


Fig. 8 Simplest examples derived from the four reactions of the R_5 vector

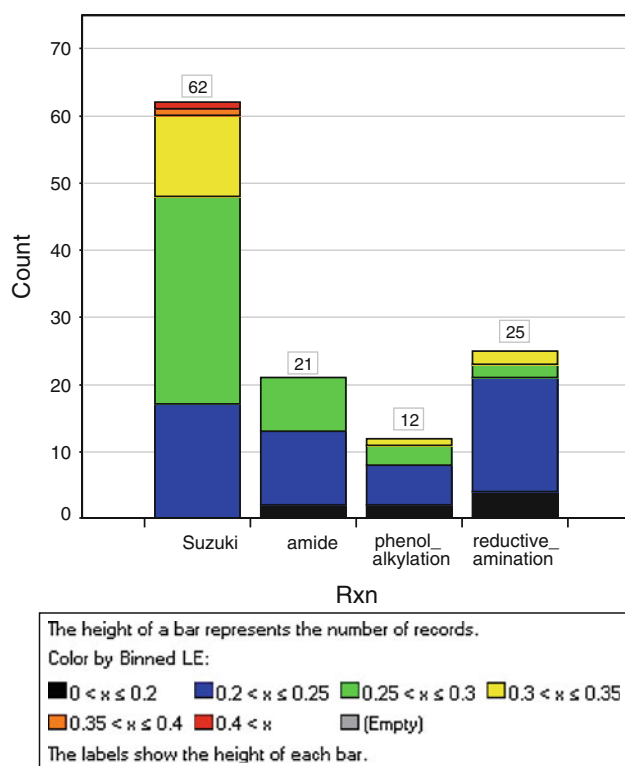


Fig. 9 Comparison of the four reaction types for the R_4 , R_5 , R_6 and R_7 vectors

phenol alkylation libraries produced some compounds with good LE, but by far, the Suzuki libraries afforded the most potent and LE isoquinolone compounds.

Probing the isoquinolone core began with the R_6 and R_7 vectors via the Suzuki reaction, and the R_6 vector produced

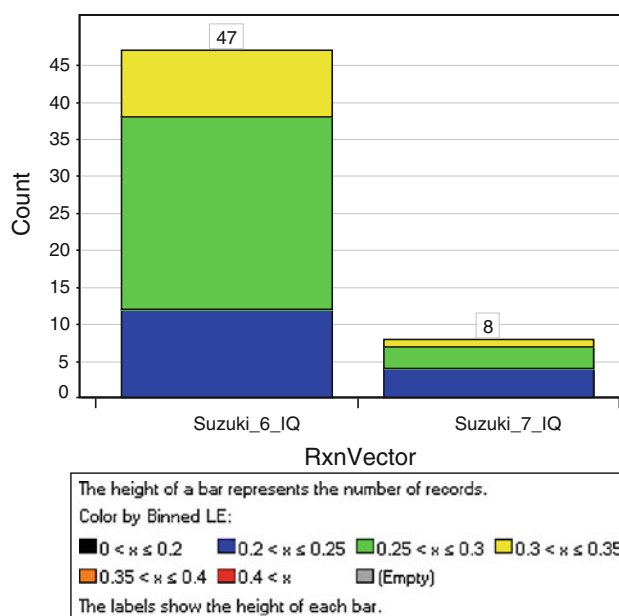


Fig. 10 Comparison of LE compounds produced via Suzuki coupling for R_6 and R_7 vectors

more potent and LE compounds (47) than the R_7 vector (8) (Fig. 10). Ten compounds with $LE > 0.3$ were prepared, and **14** was the most potent compound, $IC_{50} = 12.3 \mu M$, providing a 70 fold increase in potency over **5** (Fig. 11). Importantly, the R_7 vector was found to tolerate fairly large groups, e.g. pyrazole and p-CN-phenyl, as depicted by **17** and **18**. This data suggested that the isoquinolone core bound to the hinge in the “Flipped In” mode. In addition, this library afforded benzyl alcohols **15** and **16** that both exhibited improved potency coupled with good measured solubility, characteristics necessary for crystallographic determination.

We were quite pleased to obtain an X-ray crystal structure of **16** in complex with the PDK1 kinase domain (Fig. 12). In this structure (PDB code 3SC1), the isoquinolone bound to the hinge region, and the first hydrogen bond was established between the carbonyl O of the isoquinolone with the backbone NH of the Ala-162. An additional hydrogen bond was observed between the N2 N of the isoquinolone with the backbone carbonyl of Ser-160. The two aryl groups were twisted allowing the benzylic alcohol to form a hydrogen bond with Glu-166. This structure confirmed the “Flipped In” binding orientation, and predicted that growth off of the R_4 , R_5 and R_6 vectors would provide the most productive interactions with the protein.

With the confirmation of the “Flipped In” binding mode, the nitrile of **14** was also suspected to interact with Glu-166, as was the case with the benzyl alcohol of **16**. In order to increase the interaction as well as to enhance

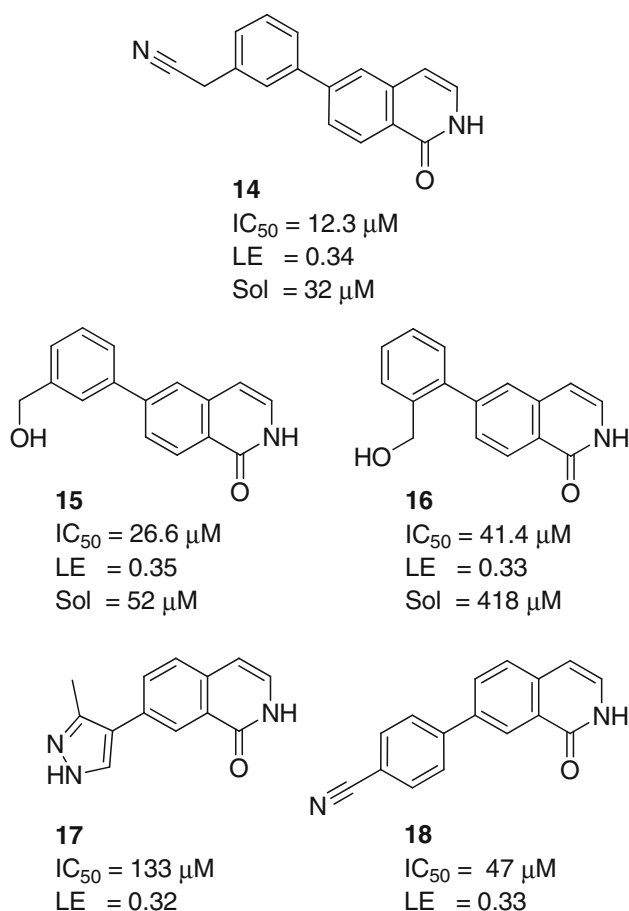


Fig. 11 Example isoquinolones derived from Suzuki coupling at R_6 and R_7

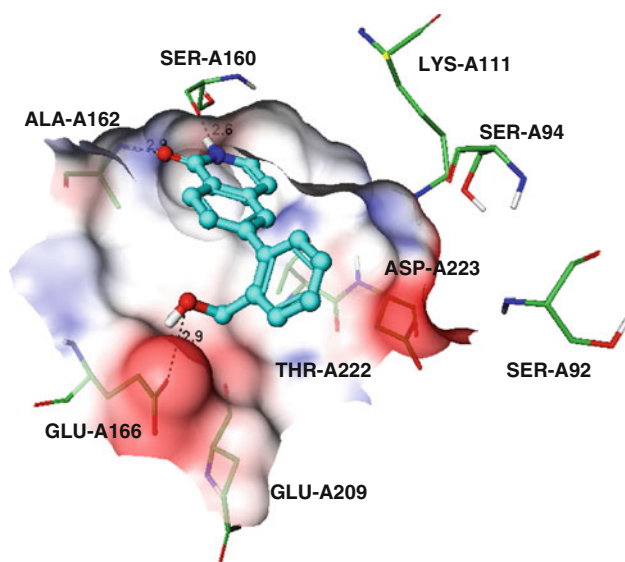


Fig. 12 Co-crystal structure of compound **16** bound to PDK1 (PDB code 3SC1)

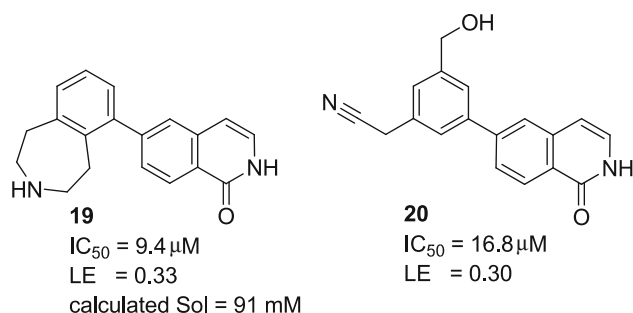


Fig. 13 Isoquinolones derived from R_6 vector

solubility for crystallographic reasons, the nitrile was reduced to the amine and tied back to the phenyl group to afford **19** (Fig. 13). Compound **19** was the first example of a compound with less than $10 \mu M$ potency and greater than 0.3 LE in the isoquinolone series. Although the calculated solubility was excellent for **19**, no crystal structure was obtained for this compound. In an effort to access the G-loop, the two pendant side-chains of **14** and **15** were simultaneously appended so that the nitrile would interact with Glu-166 while the benzylic alcohol would reach back to Ser-94. Disappointingly, this compound did not afford the additional expected potency boost. Although docking scoring indicated otherwise, perhaps neither the benzylic alcohol nor the nitrile were optimally aligned for good, simultaneous interactions with Glu-166 and Ser-94.

Efforts turned to exploring the R_4 and R_5 vectors through Suzuki coupling. As expected, the R_4 vector was intolerant of large groups (data not shown). On the other hand, the R_5 vector produced the most potent and ligand efficient compounds of all the vectors explored (Fig. 14). Compounds **21–23** represented an interesting series; additional methyl groups appended to the pyrazole caused unfavorable twisting between the two rings, giving a drop in potency. Compound **24** was the most potent and ligand efficient compound optimized for the isoquinolone series, with almost a 500 fold increase in potency and increased LE from the original isoquinolone fragment **5**. For unknown reasons, all attempts to crystallize **24** with PDK1 were unsuccessful. The docking experiments suggested **24** was still forming the pair of key hydrogen bonds between the carbonyl O of the isoquinolone with the backbone NH of the Ala-162 and the N2 N of the isoquinolone with the backbone carbonyl of Ser-160, but the isoquinolone motif had shifted in the hinge compared to **16** (Fig. 15). Despite the lack of crystallographic information, **24** was an attractive lead series with orthogonal risk profile to the HTS series with greater than five-fold selectivity against other key pathway kinases, PI3K, S6K, AKT and CDK, (<20% Inhibition @ $10 \mu M$).

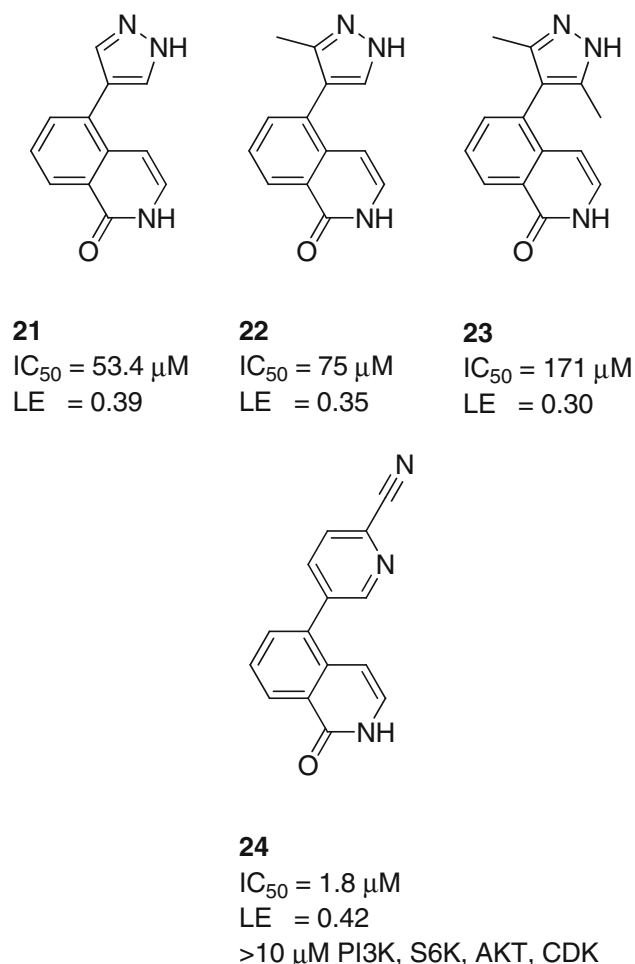


Fig. 14 Isoquinolones derived from Suzuki coupling at R₅

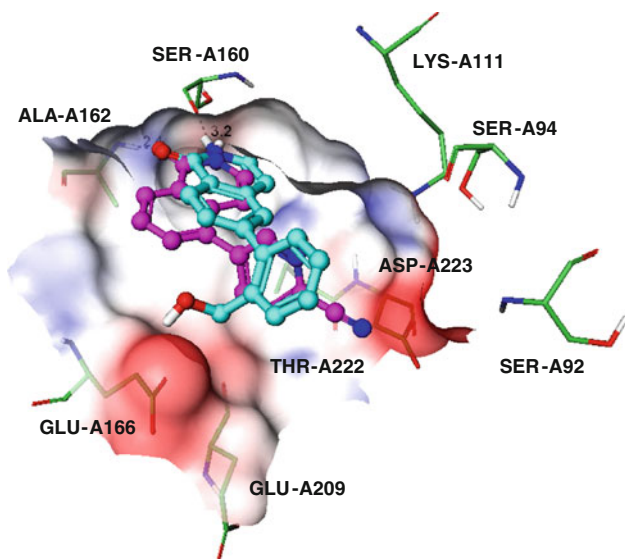


Fig. 15 Docked **24** (magenta) into the PDK1 crystal structure for **16** (cyan)

Conclusions

In conclusion, NMR screening of ~10,000 fragments followed by a biochemical assay provided a useful starting point for the back-up PDK1 fragment effort. Effective hit triage involved quick SAR mining; however, the number of small, common structural motifs lacking from commercial vendors was surprising. Clearly, carefully designed fragment libraries coupled with continuously filling the corporate collection with unique, follow-up compounds would fast-forward any fragment effort [27]. Additional orthogonal assay testing, e.g. SPR or MS, would have been helpful to detect promiscuous binders as well as compounds missed in the biochemical or NMR assay. If no crystal structure of a fragment hit bound to the protein existed, then prioritizing work on fragments with the highest LE (ideally > 0.35) gave the most promising results. Although having a fragment crystal structure would clearly be advantageous, fragments leads were advanced using known crystal structures of other ligands bound to the protein coupled with utilizing parallel synthesis methods to quickly explore available vectors. Combinatorial expansion made an excellent tool for quickly growing fragment leads, as many of the fragments themselves were monomers and readily available as starting materials. This technique provided a 500 fold increase in potency with increased LE in one synthetic step from the original fragment, thereby quickly affording a good candidate for lead optimization.

References

1. Rees DC, Congreve M, Murray CW, Carr R (2004) Fragment-based lead discovery. *Nat Rev Drug Discov* 3:660–672
2. Jahnke W, Erlanson DA (eds) (2006) Fragment-based approaches in drug discovery. Wiley, New York
3. Hajduk PJ, Greer J (2007) A decade of fragment-based drug design: strategic advances and lessons learned. *Nat Rev Drug Discov* 6:211–219
4. Congreve M, Murray CW, Carr R, Rees DC (2007) Fragment-based lead discovery. In: Macor JE (ed) *Annual Reports in Medicinal Chemistry* 42:431–448
5. Congreve M, Chessari G, Tisi D, Woodhead AJ (2008) Recent developments in fragment-based drug discovery. *J Med Chem* 51:3661–3680
6. Hopkins AL, Groom CR, Alex A (2004) Ligand efficiency: a useful metric for lead selection. *Drug Discov Today* 9:430–431
7. Peifer C, Alessi DR (2008) Small-molecule inhibitors of PDK1. *Chem Med Chem* 3:1810–1838
8. Mora A, Komander D, van Aalten DMF, Alessi DR (2004) PDK1, the master regulator of AGC kinase signal transduction. *Cell Dev Biol* 15:161–170
9. Tokar A, Newton AC (2000) Cellular signaling: pivoting around PDK-1. *Cell* 103:185–188
10. Bayascas JR, Leslie NR, Parsons R, Fleming S, Alessi DR (2005) Hypomorphic mutation of PDK1 suppresses tumorigenesis in PTEN^{+/-} Mice. *Curr Biol* 15:1839–1846

11. Angiolini M, Banfi P, Casale E, Casuscelli F, Fiorelli C, Saccardo MB, Silvagni M, Zuccotto F (2010) Structure-based optimization of potent PDK1 inhibitors. *Bioorg Med Chem Lett* 20:4095–4099
12. Nittoli T, Dushin RG, Ingalls C, Cheung K, Floyd MB, Fraser H, Olland A, Hu Y, Grosu G, Han X, Arndt K, Guo B, Wissner A (2010) The identification of 8, 9-dimethoxy-5-(2-aminoalkoxy-pyridin-3-yl)-benzo[c][2,7]naphthyridin-4-ylamines as potent inhibitors of 3-phosphoinositide-dependent kinase-1 (PDK-1). *Eur J Med Chem* 45:1379–1386
13. Stauffer F, Maira S-M, Furet P, García-Echeverría C (2008) Imidazo[4,5-c]quinolines as inhibitors of the PI3K/PKB-pathway. *Bioorg Med Chem Lett* 18:1027–1030
14. Hubbard RE, Davis B, Chen I, Drysdale MJ (2007) The seeds approach: integrating fragments into drug discovery. *Curr Top Med Chem* 7:1568–1581
15. Medina JR, Blackledge CW, Heerding DA, Campobasso N, Ward P, Briand J, Wright L, Axten JM (2010) Aminoindazole PDK1 Inhibitors: a case study in fragment-based drug discovery. *ACS Med Chem Lett* 1:439–442
16. Medina JR, Becker CJ, Blackledge CW, Duquenne C, Feng Y, Grant SW, Heerding D, Li WH, Miller WH, Romeril SP, Scherzer D, Shu A, Bobko MA, Chadderton AR, Dumble M, Gardiner CM, Gilbert S, Liu Q, Rabindran SK, Sudakin V, Xiang H, Brady PG, Campobasso N, Ward P, Axten JM (2011) Structure-based design of potent and selective 3-phosphoinositide-dependent kinase-1 (PDK1) inhibitors. *J Med Chem* 54:1871–1895
17. Erlanson DA, Arndt JW, Cancilla MT, Cao K, Elling RA, English N, Friedman J, Hansen SK, Hession C, Joseph I, Kumaravel G, Lee W-C, Lind KE, McDowell RS, Miatkowski K, Nguyen C, Nguyen TB, Park S, Pathan N, Penny DM, Romanowski MJ, Scott D, Silvian L, Simmons RL, Tangonan BT, Yang W, Sun L (2011) Discovery of a potent and highly selective PDK1 inhibitor via fragment-based drug discovery. *Bioorg Med Chem Lett* 21:3078–3083
18. Stockman BJ, Kothe M, Kohls D, Weibley L, Connolly BJ, Sheils AL, Cao Q, Cheng AC, Yang L, Kamath AV, Ding Y-H, Charlton ME (2009) Identification of allosteric PIF-pocket ligands for PDK1 using NMR-based fragment screening and ^1H – ^{15}N TROSY experiments. *Chem Biol Drug Des* 73:179–188
19. Mayer M, Meyer B (1999) Characterization of ligand binding by saturation transfer difference NMR spectroscopy. *Angew Chem Int Ed* 38:1784–1788
20. <http://accelrys.com/products/datasheets/accord-chemistry-cartridge.pdf>
21. Hajduk PJ (2006) Fragment-based drug design: how big is too big? *J Med Chem* 49:6972–6976
22. Pipeline Pilot from Accelrys: <http://www.accelrys.com/>
23. Gehlhaar DK, Verkhivker GM, Rejto PA, Sherman CJ, Fogel DB, Fogel LJ, Freer ST (1995) Molecular recognition of the inhibitor AG-1343 by HIV-1 protease: conformationally flexible docking by evolutionary programming. *Chem Biol* 2:317–324
24. Gehlhaar DK, Bouzida D, Rejto PA (1999) Reduced dimensionality in ligand-protein structure prediction: covalent inhibitors of serine proteases and design of site-directed combinatorial libraries. In: Parrill AL, Reddy MR (eds) *Rational drug design: novel methodology and practical applications*. ACS Symposium Series, ACS Press, New York, 719:292–311
25. Marrone TJ, Luty BA, Rose PW (2000) Discovering high-affinity ligands from the computationally predicted structures and affinities of small molecules bound to a target: a virtual screening approach. *Perspect Drug Discov Des* 20:209–230
26. Fish PV, Barber CG, Brown DG, Butt R, Collis MG, Dickinson RP, Henry BT, Horne VA, Huggins JP, King E, O’Gara M, McCleverty D, McIntosh F, Phillips C, Webster R (2007) Selective urokinase-type plasminogen activator inhibitors. 4.1-(7-Sulfonamidoisoquinolinyl)guanidines. *J Med Chem* 50:2341–2351
27. Lau WF, Withka JM, Hepworth D, Magee TV, Du YJ, Bakken GA, Miller MD, Hendsch ZS, Thanabal V, Kolodziej SA, Xing L, Hu Q, Narasimhan LS, Love R, Charlton ME, Hughes S, Van Hoom WP, Mills JE (2011) Design of a multi-purpose fragment screening library using molecular complexity and orthogonal diversity metrics. *J Comput-Aided Mol Des* (in press)